Crossover from classical to relaxor ferroelectrics in $BaTi_{1-x}Hf_xO_3$ ceramics

2006 J. Phys.: Condens. Matter 18 3455

(http://iopscience.iop.org/0953-8984/18/13/013)

INSTITUTE OF PHYSICS PUBLISHING JOURNAL OF PHYSICS: CONDENSED MATTER

J. Phys.: Condens. Matter **18** (2006) 3455–3468 doi:10.1088/0953-8984/18/13/013

Crossover from classical to relaxor ferroelectrics in $BaTi_{1-x}Hf_xO_3$ ceramics

Shahid Anwar, P R Sagdeo and N P Lalla

UGC-DAE Consortium for Scientific Research, University Campus, Khandwa road, Indore, 452017, India

Received 31 December 2005
Published 14 March 2006
Online at stacks.iop.org/JPhysCM/18/3455

Abstract

In this paper we report the successful preparation of hafnium substituted barium titanate, i.e. $BaTi_{1-x}Hf_xO_3$ (BHT) ceramics with ($x = 0.05, 0.1, 0.2, 0.3$ and 0.4). X-ray diffraction measurements followed by Reitveld analysis show the single-phase nature of these ceramics undergoing a tetragonal to cubic phase transformation for $x \geqslant 0.10$. Temperature dependent dielectric properties (ε' and ε'') of these single-phase BHT ceramics have been studied in the temperature range 90–375 K and frequency range 0.1–100 kHz. Dispersionless but hysteric ε'–T and ε''–T behaviour has been observed for $x < 0.3$ whereas for $x \geqslant 0.3$ highly diffusive and depressive ε'–T and ε''–T behaviour has been observed. The three different phase transitions of pure $BaTiO_3$ get pinched into a single diffused round peak along with frequency dispersion for $x \geqslant 0.3$. This clearly indicates an evolution of classical to relaxor ferroelectrics crossover with increasing x in these BHT ceramics. The parameters characterizing the relaxor behaviour have been analysed. The mechanism for the dielectric relaxation process and pinching of phase transition and their effect on ferroelectric behaviour is discussed.

1. Introduction

Perovskite-based oxides have attracted considerable interest owing to the rich diversity of their physical properties and possible technological applications [1, 2]. The reasons for their broad application include their stability over a wide temperature range, low cost, and ease with which the composition and microstructure can be optimized and tailored for specific applications [3, 4]. The ferroelectric relaxors observed in mixed perovskites are examples of one such oxide and bears special importance [1, 5]. The promising electrical properties [3, 6] of these materials have given thrust to carry out fundamental and applied research on relaxor ferroelectrics.

Most of the known ferroelectric relaxors belong to the family of lead-based perovskites, such as $Pb(Mg_{1/3}Nb_{2/3})O_3$(PMN), $Pb(Sc_{1/2}Ta_{1/2})O_3$(PST), *and* (PbLa)$(ZrTi)O_3$ (PLZT) [5–7],

with more than one type of ion occupying different equivalent crystallographic sites [6, 7]. However, these composition have drawbacks like the volatility and toxicity of Pb, and thus with increasing demand for environmental protection, lead-free materials are highly desirable. Studies based on environmentally friendly applications (dielectrics for capacitors, actuators, etc) have therefore been performed in detail on different lead-free ceramics, such as $BaTiO_3$ and its doped versions such as Ca, Sr, Ce, Sn doped at A or B sites of the ABO_3 perovskite structure [8–11]. Of these, the Ba(Ti-Zr)O_3(BZT) based materials have shown promising properties as future lead-free materials [10, 12]. These materials are either classical or relaxor ferroelectrics depending on the level of substitution [8, 12]. The main features of relaxors are connected to their structural and compositional inhomogeneity occurring due to random site disorder [7] giving rise to the occurrence of polar nanodomains [6, 7]. The consequence of these random site impurities is the broadening of dielectric permittivity versus temperature variation. With increasing concentration of random site impurity smearing also increases, which has been attributed [7, 8] to the presence of microregions with local compositional variation with respect to the average composition. These different microregions are assumed to transform at different temperatures and hence the transformation takes place over a wide range of temperature called the 'Curie range', leading to a diffuse phase transition (DPT). Further it also shows a deviation [13] from the Curie–Weiss behaviour above the peak temperature of the DPT. The evolution DPT inducing a possible transition from a classical to relaxor ferroelectric as a function of substitution is worth studying in even newer materials.

The present investigation is aimed at studying the classical to relaxor ferroelectric crossover in a new lead-free composition, namely $BaTi_{1-x}Hf_xO_3$. The extreme members of this series, i.e. $BaTiO_3$ and $BaHfO_3$, are reported to be tetragonal ferroelectric [14] and cubic paraelectric [15] at room temperature. A detailed study of the variation of structural and dielectric properties corresponding to different Hf concentrations at the Ti site at various temperatures and frequencies is presented. An extensive literature survey suggested that no such detailed report to our knowledge has been made on Hf-substituted $BaTiO_3$.

2. Experimental details

Various compositions of $BaTi_{1-x}Hf_xO_3$ ceramics, with $x = 0.05, 0.1, 0.2, 0.3$ and 0.4, were prepared via the conventional solid-state reaction technique. High-purity (99.99%) powders of $BaCO_3$, TiO_2 and HfO_2 were weighed in stoichiometric proportions and wet-mixed, using acetone as the mixing medium. After well mixing and drying, the powder was calcined at 1100 °C for 6 h. The calcined powders were remixed, dried, and then palletized in a 15 mm diameter disc at 100 kN cm^{-2} pressure using polyvinyl alcohol as binder. The pallets were then sintered at 1250 °C for 12 h and cooled naturally to room temperature while the furnace power kept off.

The as-prepared samples of $Ba(Ti_{1-x}Hf_x)O_3$ were subjected to structural and phase purity characterizations using powder x-ray diffraction (XRD). The XRD measurements were carried out using Cu Kα radiation and employing a Rigaku goniometer and rotating anode x-ray generator working at 10 kW output power. Electroding of the flat surfaces of the pallets was carried out by painting the surfaces with high-temperature silver paint. The painted pallets were then dried and fired at 500 °C for 15 min before proceeding with dielectric measurements. Dielectric characterization of pallets, as a function of temperature, was carried out employing temperature-controlled measurement of dielectric permittivity (ε') and dielectric loss ($\tan\delta$) in temperature range of 90–375 K. For these measurements a computer interfaced and programmed LCR meter (Hioki-3538) and a temperature controller (Lakeshore) with Pt-100 as the temperature sensor was used. The Pt-100 temperature sensor was used in four-probe

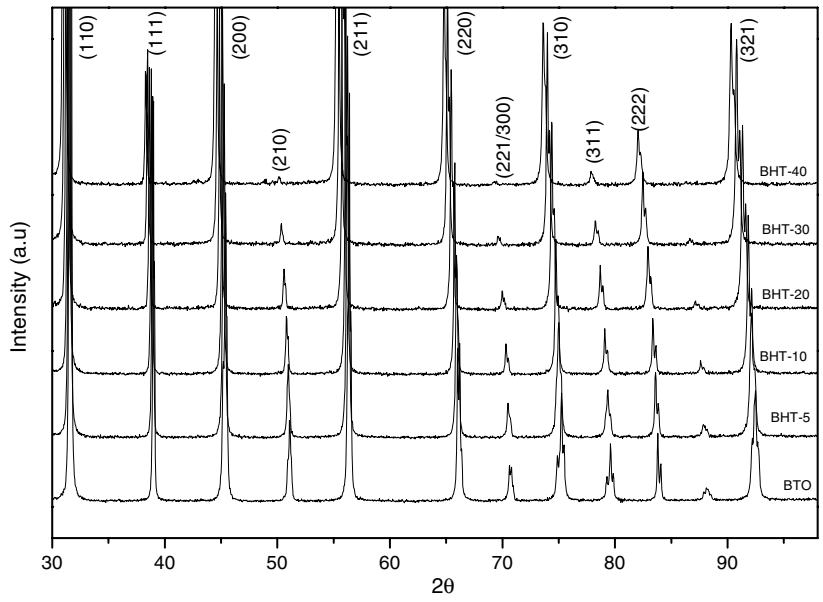

Figure 1. Room temperature x-ray diffraction profiles for $Ba(Ti_{1-x}Hf_x)O_3$ ceramics for $x = 0, 0.05, 0.10, 0.20, 0.30$ and 0.40.

mode. A peak-to-peak ac signal of 1.0 V in the frequency range 10^2–10^5 Hz and a temperature step of 0.5 K with set-point stability better than 20 mK in the entire studied temperature range were used. Thus the measurement process ensures that no anomaly is left unobserved in the entire temperature range studied.

3. Results

3.1. Structural studies

Figure 1 shows x-ray diffraction patterns of ($BaTi_{1-x}Hf_xO_3$) ceramics for $x = 0, 0.05, 0.10, 0.20, 0.30$ and 0.40. In figure 1, a systematic lower angle shift of diffraction peaks with respect to $x = 0$, i.e. pure $BaTiO_3$, can be seen with increasing Hf content. This systematic change very clearly indicates that Hf has really been substituted in $BaTiO_3$. A careful observation also shows that the splitting of some of the peaks of the tetragonal $BaTiO_3$, for example (002)/(200) and (310)/(301), have merged into single peaks with Hf doping. This has been more clearly shown in figure 2 for the (002)/(200) and (310)/(301) peaks [8]. Merging of peaks indicates a phase transformation from tetragonal phase into a higher symmetry phase, most probably cubic. Shifting of peaks to the lower angle side indicates that the lattice parameters are increasing due to substitution of hafnium (Hf^{4+}), which has a larger size in comparison with titanium (Ti^{4+}). To get accurate values of lattice parameters and also to confirm the tetragonal to cubic transition with increasing Hf, we carried out Reitveld analyses of the measured XRD data. We could successfully refine the XRD data with $P4mm$ (tetragonal) and $Pm3m$ (cubic) space-groups for different values of concentration. A typical such refined XRD dataset for $x = 0.3$, whose goodness of fit is 2.5, is shown in figure 3. The inset of figure 3 shows the lattice parameter variation with Hf content. As **x** increases **c** decreases but **a** increases and at $x = 0.1$ both become equal, leading to a tetragonal to

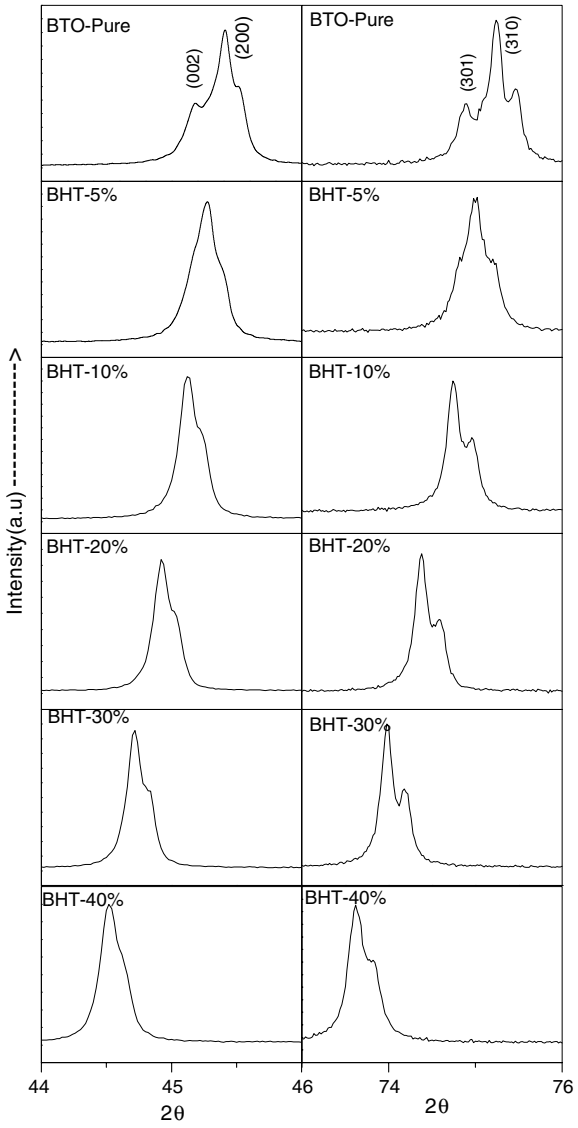

Figure 2. Enlarged view of XRD profiles of $Ba(Ti_{1-x}Hf_x)O_3$ ceramics ($x = 0, 0.05, 0.10, 0.20, 0.25, 0.30$) depicting (200)/(002) and (310)/(301) reflections.

cubic transformation. Above $x = 0.1$ the lattice parameter of the cubic phase increases almost linearly with Hf concentration. Pure $BaHfO_3$ is reported [15] to be cubic with lattice parameter 4.17 Å. Our result is in conformity with this.

The percentage densification (pallet density $\times$ 100/its x-ray density) of the pallets was also estimated using the x-ray density (calculated using the refined lattice parameter and the atomic contents) and the pallet density (calculated using the mass and the geometrical volume of the pallet). A decreasing trend of densification from 90% to 80% was observed with **x** increasing from 0.05 to 0.4. The mean grain size as measured using SEM micrographs of the pallets was found to be $\sim$5 μm for every composition.

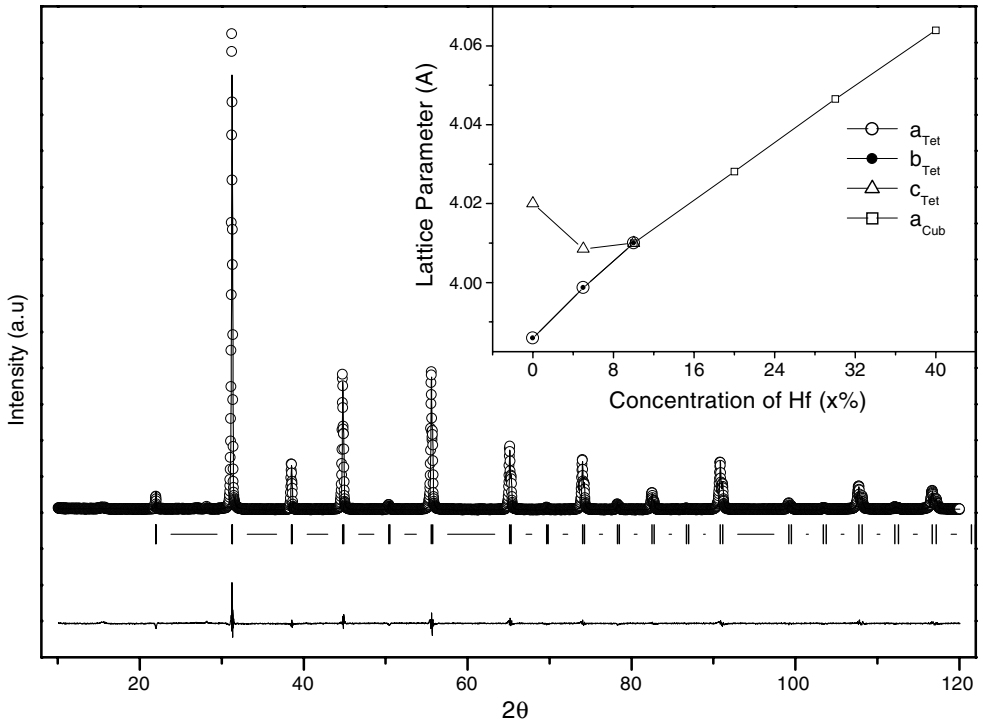

Figure 3. Representation of a typical Reitveld refined pattern of the studied BHT ceramics. The current pattern corresponds to the cubic relaxor phase (i.e. $BaTi_{0.7}Hf_{0.3}O_3$). Symbols represent the observed data points and the solid line its Reitveld fit. The inset shows the tetragonal to cubic transition and change in lattice parameter as a function of hafnium (Hf) substitution at titanium (Ti) site.

3.2. Dielectric studies

The temperature dependence of the real (ε') and imaginary (ε'') parts of the dielectric permittivity of $Ba(Ti_{1-x}Hf_x)O_3$ for $x = 0.05, 0.1, 0.2, 0.3$ and 0.4 samples is shown in figures 4(a)–(d). For each composition these measurements were made at frequencies of 0.1, 1, 10 and 100 kHz during both cooling and heating cycles. The upper insets in all panels of figure 4 represent typical examples of cooling and heating cycles. A common feature of the observed temperature variations is that ε' and ε'' both peak at a certain temperature but the sharp change in dielectric permittivity is gradually replaced by diffusive behaviour with increasing hafnium concentration. It is found that T_m, the temperature at which the ε' is maximum, decreases with hafnium concentration; see table 1 and figure 5 and the inset therein. The point corresponding to $x = 0$, i.e. the pure $BaTiO_3$ ($T_C = 393$ K), has been taken from reported literature [14]. Two distinct regions of the slope dT_m/dx have been observed, as indicated by solid lines as a guide to the eyes. The approximate values of dT_m/dx in these two regions are estimated, based on its linear fit, to be 7 and 3.5 K mol%$^{-1}$ respectively for $x = 0.05$–0.2 and $x = 0.3$–0.4.

Another important feature observed in figure 4 is that for samples with $x \leqslant 0.2$, figures 4(a) and (b), the ε'–T variations show a clear hysteresis but no frequency dispersion. But for $x \geqslant 0.30$, figures 4(c) and (d), these features are exactly opposite. ε'–T variations show no hysteresis but pronounced frequency dispersion. This strongly indicates that as a function

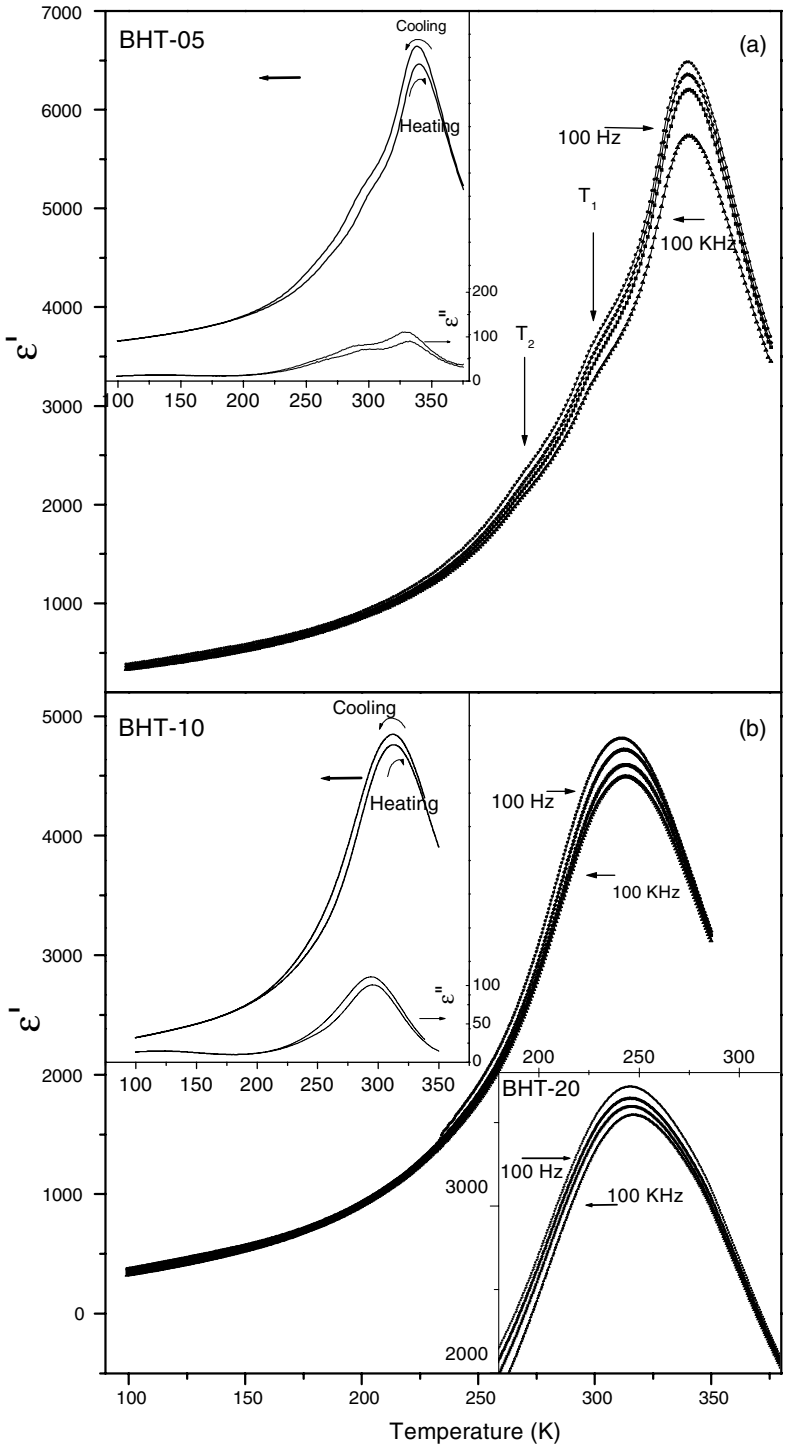

Figure 4. Temperature dependence of real (ε') and imaginary (ε'') parts of the permittivity of $Ba(Ti_{1-x}Hf_x)O_3$ ceramics for ((a), (b)) $x = 0.05, 0.10, 0.20$ and ((c), (d)) $x = 30$ and 0.40 at various frequencies. The upper insets in each panel show the data taken during heating and cooling cycles. The data corresponding to $x = 0.20$ are shown in the lower inset of (b).

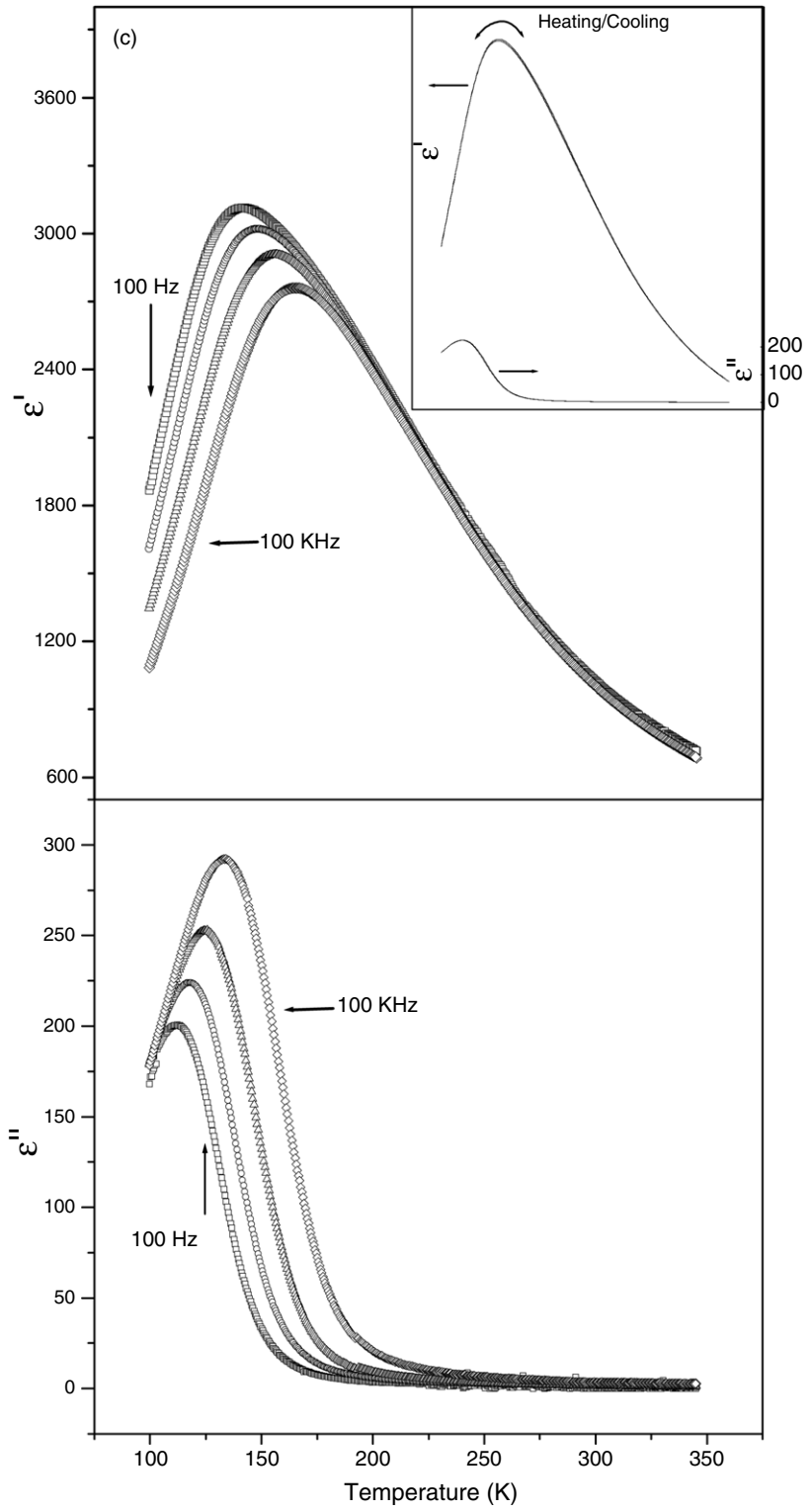

Figure 4. (Continued.)

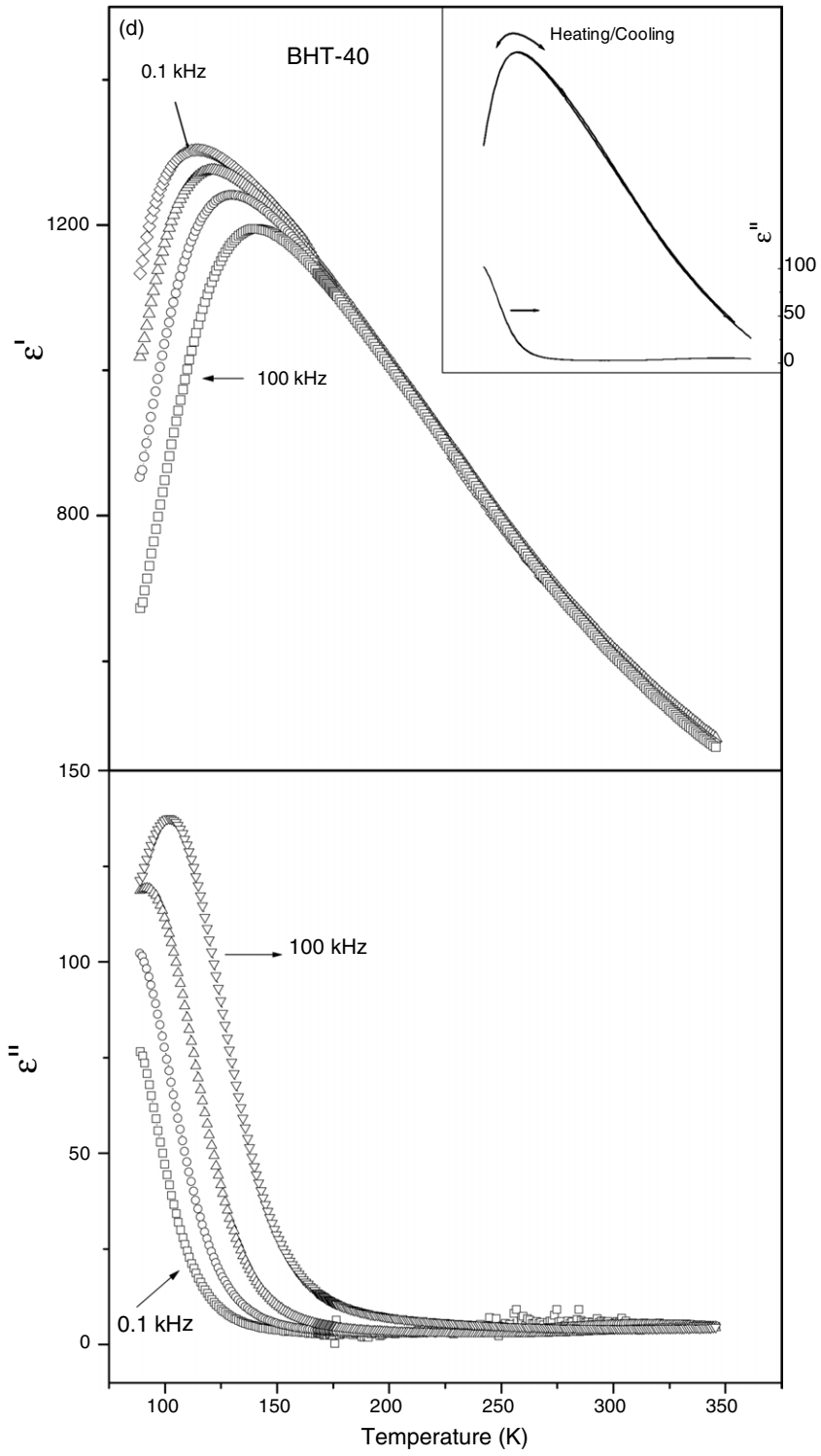

Figure 4. (Continued.)

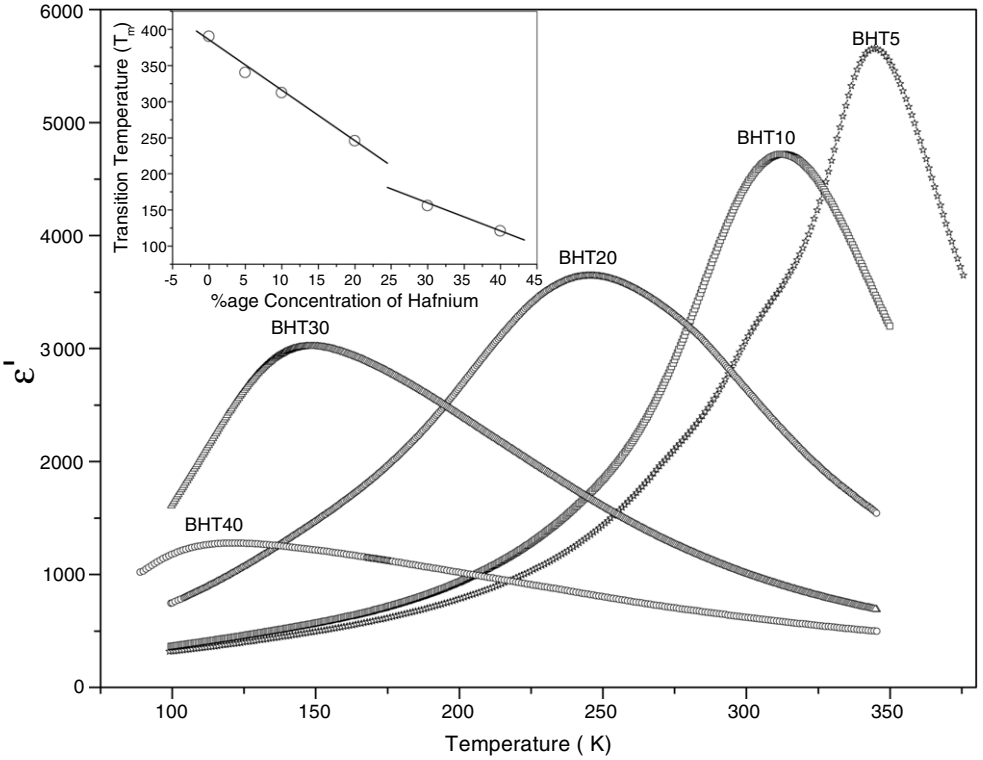

Figure 5. Comparison of temperature dependent real part of dielectric permittivity of $Ba(Ti_{1-x}Hf_x)O_3$ ceramics for $x = 0.05, 0.10, 0.20, 0.30$ and 0.40 at 1 kHz. The inset shows the variation of transition temperature (T_m) with hafnium concentration.

Table 1. Table showing parameters related to ferroelectric and relaxor behaviour. Here T_m (or T_C), ΔT_m, and ΔT_{relax} represent the transition temperature, degree of Curie–Weiss deviation, and degree of relaxation, respectively, for $Ba(Ti_{1-x}Hf_x)O_3$.

	X				
	0.05	0.10	0.20	0.30	0.40
T_m or T_C (K)	340	312	245	149	121
ΔT_m (K)	16	28	71	132	172
ΔT_{relax} (K)	∼1	∼1	∼2	23	27

of Hf substitution at the Ti site, at $x = 0.3$ some characteristic change in the dielectric property takes place.

For low level doping, i.e. for $x = 0.05$, the ε'–T maximum is relatively sharp and the value of T_m (340 K) is frequency independent. ε'–T variation shows two other anomalies at T_1(300 K) and T_2(268 K). The dielectric peak and these anomalies originate from structural phase transitions from paraelectric cubic phase to ferroelectric tetragonal phase (hence $T_m = T_C$, the Curie temperature) and then to an orthorhombic ferroelectric (at T_1) and finally to rhombohedral ferroelectric (at T_2). The T_C value corresponding to the paraelectric to ferroelectric transition gets shifted to a lower temperature and T_1 and T_2 to higher temperatures [8, 11] on substitution of Hf^{4+} at the Ti^{4+} site. This is the so-called pinching of

transitions as observed in Ca, Zr, Ce, and Sn substituted $BaTiO_3$ [8–11]. All these observations point to classical ferroelectric behaviour for $x \leqslant 0.05$ as found in pure $BaTiO_3$.

For $Ba(Ti_{1-x}Hf_x)O_3$ compositions corresponding to $0.10 \leqslant x \leqslant 0.20$ the three phase transitions get pinched and only one peak remains at the Curie temperature T_C. Figures 4(b) and (c) show the temperature and frequency dependence of ε'. There is no frequency dispersion: the value of ε' is coincident at every frequency measured. However, the peak of ε' is broader than that of for $x = 0.05$, and there is a small deviation from the Curie–Weiss law in the paraelectric phase. Such a behaviour accompanied by the hysteresis indicates that although the transition is relatively diffuse the observed behaviour corresponds to a ferroelectric phase transition only.

On increasing the substitution level of $Ba(Ti_{1-x}Hf_x)O_3$ up to $x \geqslant 0.30$, only one broad peak occurs at T_m, with frequency dispersion at temperatures below T_m ($T < T_m$) for the real part and at $T > T_m$ for the imaginary part. T_m was found to shift to higher values and ε' is decreased as the frequency increases. The value of ε' and T_m further decreases for $x = 0.4$ concentration. The value of T_m is frequency dependent, unlike that of T_C, as in classical ferroelectrics. The temperature T_m of the ε'' maximum shifts to higher values at higher frequencies, but in contrast to the evolution of ε', the ε'' maximum increases with the frequency. In addition there is a large amount of deviation from the Curie–Weiss law, which is generally observed for a classical ferroelectric. The observed temperature and frequency dependence of ε' and ε'' is specific to a ferroelectric relaxor behaviour [6, 16–19].

4. Discussion

It is well known that the dielectric permittivity of a classical ferroelectric above the Curie temperature follows the Curie–Weiss law described by

$$1/\varepsilon' = (T - T_C)/C \qquad (T > T_C), \tag{1}$$

where T_C is the Curie temperature and C is the Curie–Weiss constant. But in substituted ferroelectrics like PMN, deviation from the above Curie–Weiss behaviour has been observed [13]. The occurrence of deviation has been attributed to short-range correlation between the nanopolar domains [13]. As the level of substitution increases the deviation from Curie–Weiss law behaviour also increases. An empirical parameter ΔT_m, defined as $\Delta T_m = T_{dev} - T_m$, is often used as a measure of the degree of deviation from the Curie–Weiss law. Here T_{dev} is the deviated Curie–Weiss temperature. Since the ε'–T measurements in the present study do not extend to sufficiently high temperature, T_{dev} could not be estimated accurately. The value of T_{dev} and hence ΔT_m estimated from these data is slightly underestimated, but the increasing trend of this underestimated ΔT_m, as shown in table 1, clearly indicates the increasing deviation from Curie–Weiss behaviour with Hf concentration. Yet another parameter, the degree of relaxation ΔT_{relax}, defined as $\Delta T_{relax} = T\varepsilon'_{m(100\ kHz)} - T\varepsilon'_{m(100\ Hz)}$, has been discussed in the literature [9, 10]. Here $T\varepsilon'_{m(100\ kHz)}$ and $T\varepsilon'_{m(100\ Hz)}$ are the maximum temperatures of ε'–T measurements done at 100 kHz and 100 Hz respectively. The estimated values of ΔT_{relax} for the present measurements have been presented in table 1. These empirical parameters show that ε'–T for the composition range $x \leqslant 0.05$ follows a Curie–Weiss law, with a little deviation. For the composition range $0.05 \leqslant x \leqslant 0.20$ a large deviation from Curie–Weiss law is observed; however, the frequency dispersion (ΔT_{relax}) is almost absent. But a large deviation from the Curie–Weiss law accompanied by strong frequency dispersion (large ΔT_{relax}) in both real and imaginary parts of permittivity is observed for the compositions $x = 0.30$ and 0.4. This observation indicates that the system has become a relaxor ferroelectric for these compositions.

A modified Curie–Weiss law has been proposed by Uchino and Nomura [20] to describe the diffuseness of the phase transition as

$$1/\varepsilon' - 1/\varepsilon'_{\mathrm{m}} = (T - T\varepsilon'_{\mathrm{m}})^{\gamma}/C_1 \qquad (T > T_{\mathrm{m}}) \tag{2}$$

where γ and C_1 are modified constants, with $1 \leqslant \gamma \leqslant 2$. The value of the parameter γ gives information about the character of the phase transition. Its limiting values are $\gamma = 1$ and $\gamma = 2$. The value of γ is 1 for the case of a normal ferroelectric and a quadratic dependence (i.e. $\gamma = 2$) is valid for an ideal ferroelectric relaxor [5, 9, 21]. Thus the value of γ also characterizes the relaxor behaviour. A plot of $\ln(1/\varepsilon' - 1/\varepsilon'_{\mathrm{m}})$ as a function of $\ln(T - T\varepsilon'_{\mathrm{m}})$ is shown in figure 6. By fitting this with equation (2), the exponent γ, determining the degree of the diffuseness of the phase transition, is obtained from the slope of the $\ln(1/\varepsilon' - 1/\varepsilon'_{\mathrm{m}})$ versus $\ln(T - T\varepsilon'_{\mathrm{m}})$ plot. We obtained the value of the parameter γ to be $\sim$1.88 for both $x = 0.3$ and 0.4. The large value of $\Delta T_{\mathrm{relax}}$, and $\gamma = 1.88$, suggest that $Ba(Ti_{1-x}Hf_x)O_3$ becomes a relaxor ferroelectric at $x \geqslant 0.3$ [10, 21]. The value of γ reported for $Ba(Ti_{0.7}Zr_{0.3})O_3$ is 1.87 [10].

The frequency dispersion of the ε'–T maxima in relaxor ferroelectrics has been attributed to the distribution of relaxation times. A large number of theoretical models have been proposed to understand the diffusiveness and the dispersion. Among these the Vogel–Fulcher model has been considered to be the most successful mathematical representation for the divergent nature of relaxation time below a certain temperature [22]. The frequency dependence of the maximum temperature T_{m} of the imaginary part of the permittivity for the relaxor phase $Ba(Ti_{0.7}Hf_{0.3})O_3$ is shown in figure 7 as an $\ln(f)$ versus $1000/T_{\mathrm{m}}$ plot [10]. The observed frequency dependence of T_{m} can be described by Vogel–Fulcher's empirical relation as

$$\log f = \log f_o - E_{\mathrm{a}}/k_{\mathrm{B}}(T_{\mathrm{m}} - T_{\mathrm{f}}) \tag{3}$$

where E_{a} is the activation energy, T_{f} the freezing temperature of the polarization fluctuation, and the pre-exponential factor f_o is the Debye frequency. As the temperature is lowered, the relaxation time increases and at the critical temperature T_{f}, it becomes extremely large, and consequently the fluctuation in polarization gets frozen to a glassy state [23]. An analogous phenomenon is also observed in spin-glass systems [24]. Excellent fitting of the Vogel–Fulcher relation with the experimental data successfully explains the relaxor behaviour. The values of E_{a}, T_{f} and f_o for $Ba(Ti_{0.7}Hf_{0.3})O_3$ are found to be 0.14 eV, 78.5 K and 1.53×10^{13} Hz, respectively, which are also consistent with the earlier reports of the similar system $Ba(Ti_{0.7}Zr_{0.3})O_3$ [10].

Keeping in view the same mean grain size of $\sim$5 μm for each composition, the observed relaxor behaviour appears to arise mainly due to Hf substitution at the Ti site. Although the physical mechanism of the occurrence of relaxor behaviour is not yet fully understood, the existence of nanopolar domains in the materials is recognized to play an important role. Substitution of Ti^{4+} by Zr^{4+} in the well-known classical ferroelectric $BaTiO_3$ leads to a decrease in the Curie temperature, which is related to the fact that the ionic radius of Zr^{4+} (0.072 nm) is greater than that of Ti^{4+} (0.0605 nm) [25]. A similar kind of anomaly is expected here also, when Hf^{4+} replaces Ti^{4+}. The observed decrease in the permittivity value (at T_{m}) appears to be mainly due to Hf substitution. But the effect of decreasing densification on the measured permittivity cannot be denied. As a rough approximation, a decrease in densification from 90% to 80% is expected to give a 10% lower value of the actual permittivity. The value of T_{C} decreases drastically as Hf is substituted for Ti. This variation of T_{C} is related to the size of Hf^{4+}, which is larger than Ti^{4+} (for six-fold coordination); as a result of substitution the shift (Δz) of the tetravalent cation from the oxygen octahedra centre becomes limited, which causes lowering of the transition temperature T_{C} [10, 11, 26]. The observed decrease of T_{C} (T_{m}) as shown in figure 5 having two different slopes $\mathrm{d}T_{\mathrm{m}}/\mathrm{d}x$ has also been reported earlier for Sr–K–(Nb–Ta)–O, Ba–Na–Nb–O–F [27] and Ba–Ti–Ce–O [9] systems, which also exhibit a normal

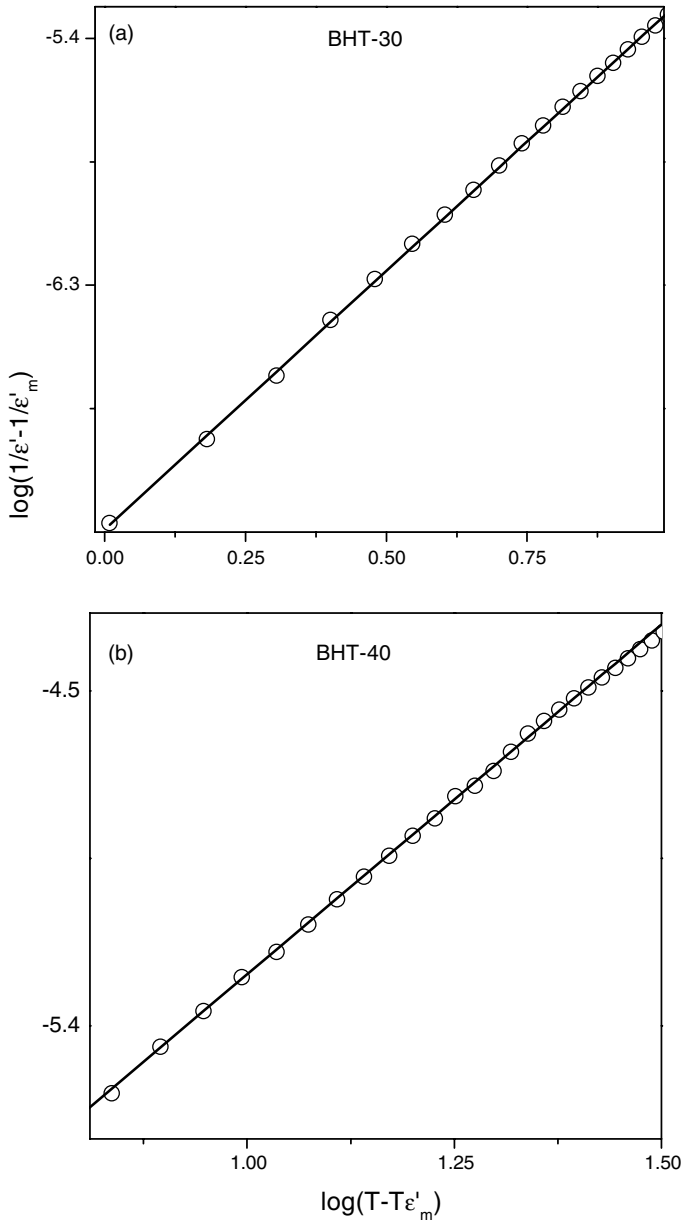

Figure 6. Log $(1/\varepsilon' - 1/\varepsilon'_{\mathrm{m}})$ versus log $(T - T\varepsilon'_{\mathrm{m}})$ plots for $x = 0.3$ and 0.4 BHT ceramics at 10 KHz. Symbols represent the experimental data and the solid line is the linear fit.

to relaxor ferroelectric crossover. In every case the changeover in the slope takes place exactly at the changeover point of normal to relaxor ferroelectric. This is what has also been observed in the present study on BHT ceramics. Thus it appears that the observed changeover in $\mathrm{d}T_{\mathrm{m}}/\mathrm{d}x$ slope is a characteristic of a normal to relaxor ferroelectric phase transition. Initially for a small amount of substitution, a diffusive type of phase transition but no signature of relaxor phase appears. Since both the substituents in the six-fold coordination site have equal charge,

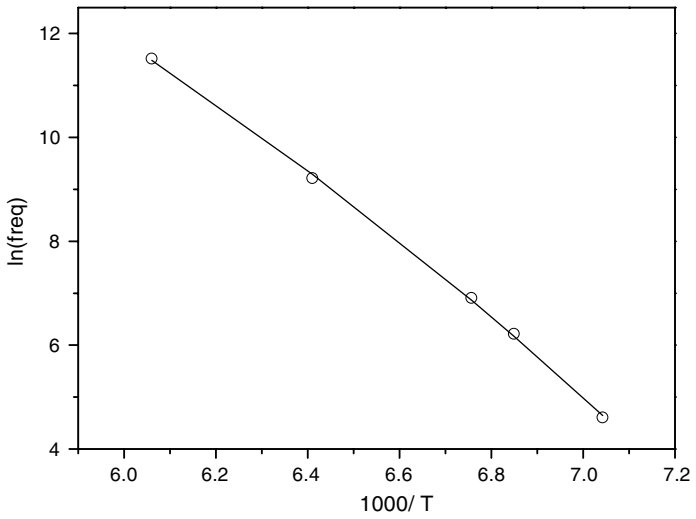

Figure 7. Frequency dependence of T_m for $Ba(Ti_{0.7}Hf_{0.3})O_3$ ceramics. The symbols and solid line indicate data points and the fit to Vogel–Fulcher's relation, respectively.

these cations require a large amount (∼30%) of Hf substitution to induce relaxor behaviour. In the case of BZT, relaxor behaviour is also reported [10] for 30% Zr substitution only.

When Hf^{4+} substitutes for Ti^{4+} the ferroelectricity and structure of the parent matrix gets modified, because Hf^{4+} ions possess larger ionic radius (0.071 nm) than Ti^{4+} (0.0605 nm). These substituents make the distance between off-centred Ti dipoles larger and larger, and thus weaken the correlation among them, which is well supported by the variation of lattice parameter (i.e. with increasing number of Hf^{4+} ions the cell volume also increases). Hence macroscopic ferroelectric domains get destroyed and nanopolar domains are formed. In other words, the crossover from the ferroelectric to diffusive relaxor transition arises due to the entering of Hf in the Ti site, disrupting the dipoles, creating a higher degree of disorder and eventually inducing relaxor behaviour. Such behaviour introduces structural randomness, lattice defects, and lattice strain; hence the symmetry breaking occurs at the nanometre scale, leading to the formation of nanopolar domains which increase in size upon cooling, but never become large enough to precipitate a long-range ordered ferroelectric state [9, 12, 21].

5. Conclusion

The dielectric behaviour of $Ba(Ti_{1-x}Hf_x)O_3$ ceramics has been studied in a wide composition range ($0 < x \leqslant 0.40$) between 90 and 375 K. A gradual evolution of a diffuse ferroelectric phase transition for $x \leqslant 0.20$ followed by pronounced dispersion in the temperature dependence of ε' and ε'' for $x \geqslant 0.30$ shows a crossover from normal to relaxor ferroelectric behaviour with increasing Hf content. The value of the exponent γ in the modified Curie–Weiss law is found to be 1.88, which remains same for $x = 0.3$ and 0.4. From the x-ray diffraction followed by Reitveld refinement of these ceramics it is concluded that Hf substitution at the Ti site causes a tetragonal to cubic transformation at around $x = 0.1$; the room temperature structure of the relaxor phase is cubic. A Vogel–Fulcher treatment of the data resulted in characteristic parameters, which are found to be in accordance with those of earlier reports.

Acknowledgments

The authors would like to acknowledge Dr P Chaddah, the Director, Professor V N Bhoraskar, the Ex-Director, and Professor Ajay Gupta, the Center Director of UGC-DAE CSR-Indore for their encouragement and interest in the work. The authors sincerely acknowledge Professor L E Cross for providing some basic references and Dr Archna Jaiswal for helping at various stages. Constant help and effort by Mr P Sarvanan and related staff for providing cryogenic liquid is gratefully acknowledged. Partial support from DST is also sincerely acknowledged.

References

[1] Mountwala A J 1971 *J. Am. Ceram. Soc.* **54** 544
[2] Buchanan R C 1986 *Ceramic Materials for Electronics* (New York: Dekker)
[3] Lines M E and Glass A M 1977 *Principles and Applications of Ferroelectrics and Related Materials* (Oxford: Oxford Press)
[4] Jaffe B, Cook W R Jr and Jaffe H 1971 *Piezoelectric Ceramics* (London: Academic)
[5] Smolenski G A and Agranovskaya A I 1958 *Sov. Phys.—Tech. Phys.* **3** 1380
Smolenski G A 1970 *J. Phys. Soc. Japan Suppl.* **28** 26
[6] Cross L E 1987 *Ferroelectrics* **76** 241
Cross L E 1994 *Ferroelectrics* **151** 305–24
[7] Settler N and Cross L E 1980 *J. Appl. Phys.* **51** 4356–60
[8] Tiwari V S, Singh N and Pandey D 1995 *J. Phys.: Condens. Matter* **7** 1441
Singh N *et al* 1996 *J. Phys.: Condens. Matter* **8** 4269
Singh N *et al* 1996 *J. Phys.: Condens. Matter* **8** 7813–27
[9] Ang C, Jing Z and Yu Z 2002 *J. Phys.: Condens. Matter* **14** 8901
Ang C, Jing Z and Yu Z 1997 *J. Phys.: Condens. Matter* **9** 3081
[10] Yu Z, Ang C, Guo R and Bhalla A S 2002 *J. Appl. Phys.* **92** 2655
[11] Ravez J, Broustera C and Simon A 1999 *J. Mater. Chem.* **9** 1609–13
[12] Simon A, Ravez J and Maglione M 2004 *J. Phys.: Condens. Matter* **16** 963–70
[13] Viehland D, Jang S J, Cross L E and Wuttig M 1992 *Phys. Rev.* B **46** 8003
[14] Hippel A V 1950 *Rev. Mod. Phys.* **22** 221
[15] Lopez Garcia A R, de la Persia P and Rodiguez A M 1991 *Phys. Rev.* B **44** 9708
[16] Lin J N and Wu T B 1990 *J. Appl. Phys.* **68** 985
[17] Lu Z G and Calvarin G 1995 *Phys. Rev.* B **51** 2694
[18] Cheng Z Y, Katiyar R S, Yao X and Guo A 1997 *Phys. Rev.* B **55** 8165
[19] Merz W J 1953 *Phys. Rev.* **91** 513
[20] Uchino K and Nomura S 1982 *Integr. Ferroelectr.* **44** 55
[21] Victor P, Ranjith R and Krupanidhi S B 2003 *J. Appl. Phys.* **94** 7702
[22] Vogel H 1921 *Z. Phys.* **22** 645
Fulcher G 1925 *J. Am. Ceram. Soc.* **8** 339
[23] Laha A and Krupanidhi S B 2003 *Mater. Sci. Eng.* B **98** 204
[24] Levt L P and Ogielski A T 1986 *Phys. Rev. Lett.* **57** 2288
[25] Shannon R D 1976 *Acta Crystallogr.* A **32** 751–67
[26] Abrahams S C, Kurtz S K and Jamieson P B 1968 *Phys. Rev.* **172** 551–3
[27] Aliouane K, Guehria Laidoudi A, Simon A and Ravez J 2005 *Solid State Sci.* **7** 1327